 PIER Photonics

(Received 4 June 2026, Accepted 10 July 2026, Scheduled 13 July 2026)

Polarization-addressable Singular Jones Metasurfaces

Haoye Qin[1,2,#], Zijin Yang[2,#], Xinyang Mu[2], Wenjing Lv[2],
Jue Li[2], Yuzhi Shi[3], Bo Li[2,4], Qinghua Song[2,4,*], and Cheng-Wei Qiu[1,5,*]

[1]*Department of Electrical and Computer Engineering, National University of Singapore, Singapore 117583, Singapore*
[2]*Tsinghua Shenzhen International Graduate School, Tsinghua University, Shenzhen 518055, China*
[3]*School of Physics Science and Engineering, Institute of Precision Optical Engineering, Tongji University, Shanghai 200092, China*
[4]*Suzhou Laboratory, Suzhou 215000, China*
[5]*National University of Singapore Suzhou Research Institute, Suzhou 215000, China*

ABSTRACT: Singular optics are commonly explored through scalar or vectorial singularities, whereas matrix-level singularities remain far less developed for wave manipulations. Here, we experimentally demonstrate polarization-addressable singular Jones metasurfaces using reflective plasmonic nanostructures. By engineering polarization conversion in the reflection subspace, the Jones matrix can be driven to a singular condition, mapping an incident polarization eigenstate to a vectorial zero output. The corresponding eigen-polarization can be addressed across the Poincaré sphere by tailoring meta-atom geometries. Encircling the singularity in a two-dimensional parameter space can yield a full 2π topological phase winding, enabling dual-channel meta-holography and vortex generation. Extreme coupling breaking further produces circularly polarized zero-output eigenstates, revealing chiral Jones singularities. These results establish singular Jones metasurfaces as a compact platform for matrix-level singular optics, polarization-selective extinction, topological wavefront shaping, and chiral light-matter interactions.

1. INTRODUCTION

Optical singularities have become a central framework for controlling light [1–5], where most demonstrations are built around scalar phase singularities or vectorial polarization singularities [6–12]. These singularities have enabled robust phase winding [13–16], structured-light generation [17, 18], metasurface holography [19–21], and chiral or topological photonic responses [22–24]. In these cases, however, the singularity is usually defined directly in an optical field, a polarization texture, or a projected output channel. A more general route is to engineer singularities at the level of the optical input-output operator [15, 25–27], where the Jones or scattering matrix possesses a zero determinant and maps a nonzero input eigenstate to a vectorial zero output. Such matrix-level singularities provide a distinct degree of freedom for wave extinction and topological wave manipulation [25, 28], yet they remain far less developed than conventional scalar and vectorial singularities.

Previous matrix-level singular responses have mainly been realized in multi-port scattering systems [29, 30], such as coherent perfect absorption (CPA), where a scattering-matrix zero is accessed by coherently injecting multiple input waves with prescribed amplitude ratios and phase delays [26, 31]. This requirement makes the response powerful for coherent control [32–34], but also increases experimental complexity and obscures the role of polarization as an addressable degree of freedom. In particular, it remains challenging to realize a compact single-beam platform in which the singularity is encoded by the Jones matrix of a metasurface and can be readily addressed across the Poincaré sphere [10, 35–37].

Here, we experimentally demonstrate polarization-addressable singular Jones metasurfaces using reflective plasmonic nanostructures. By engineering polarization conversion in the reflection subspace, we drive the Jones matrix to a singular condition and map selected nonzero incident polarization eigenstates to a vectorial zero output through the interactions between orthogonal polarization components. The zero-output eigen-polarization is tunable across the Poincaré sphere by tailoring meta-atom geometries. By encircling the singularity in a two-dimensional structural parameter space, the metasurface acquires a full 2π topological phase winding, which enables dual-channel meta-holography and optical vortex generation. With stronger coupling breaking, the eigenstate can be driven toward circular polarization, giving rise to handedness-selective chiral Jones singularities. This capability highlights a route to engineering singular optical responses directly at the Jones-matrix level, where polarization extinction, topological phase control, and chiral selectivity can be integrated within a single metasurface platform.

2. RESULTS

CPA is commonly formulated in lossy two-port scattering systems, where it is identified by a zero of the scattering-matrix determinant and can therefore be viewed as a form of matrix-level singularity. To access the associated zero-output eigenstate, excitations at two spatial ports must have a specific amplitude ratio and phase delay. This requires amplitude modulation using

* Corresponding authors: Qinghua Song (song.qinghua@sz.tsinghua.edu.cn), Cheng-Wei Qiu (chengwei.qiu@nus.edu.sg). # These authors contributed equally.

 Published by THE ELECTROMAGNETIC ACADEMY

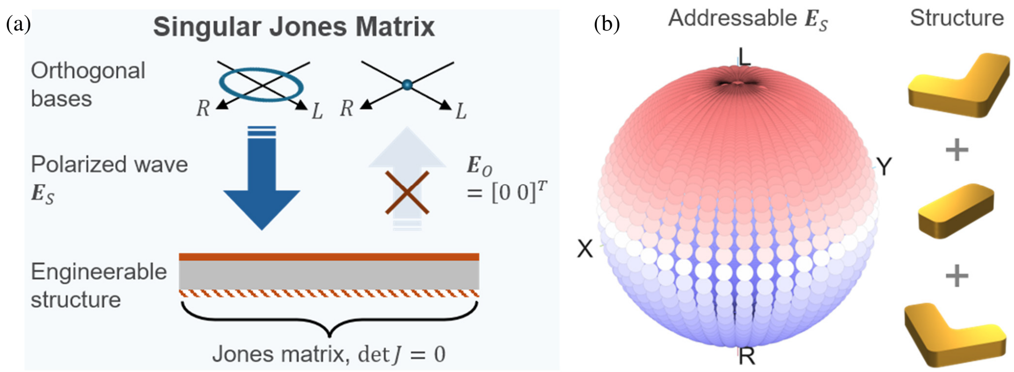

FIGURE 1. Concept of singular Jones matrix and polarization addressability. (a) Singular Jones matrix is realized in a polarization-conversion system under single-beam excitation with eigen-polarization $\mathbf{E}_S$. The outgoing vectorial zero possesses a twofold topology, appearing as a phase singularity in each basis component. (b) Engineerable plasmonic nanostructures with polarization selectivity enable such matrix-level singularity and Poincaré-sphere addressability of its eigen-polarization.

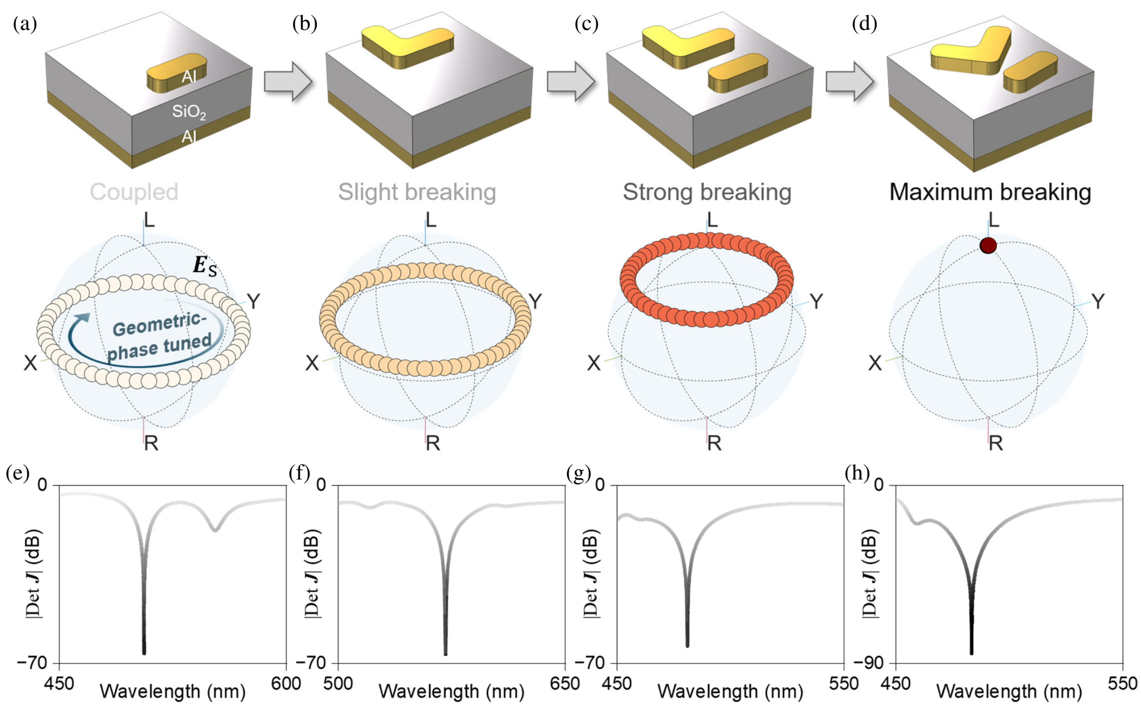

FIGURE 2. Structural design for singular Jones metasurfaces and simulated results of addressable eigen-polarization states. Engineering plasmonic geometries (rod and L shapes) and the resultant Jones coupling breaking for controllable singular eigen-polarizations, from (a) single rod, (b) L shape, to (c) coupled rod-L shape, and (d) rotated rod-L shape. The corresponding coupling-breaking levels of the Jones matrix and eigen-polarization states are shown in the bottom panels of (a)–(d), where the ideal geometric phase can operate as an encircling term. The extreme case in (d) marks chiral Jones singularity, and mirror symmetry can be used to access the opposite hemisphere. (e)–(h) Simulated spectra of Jones-matrix determinant corresponding to the structures in (a)–(d).

an attenuator or a two-arm interferometer with a tunable light path difference [27, 30, 38].

Similarly, we propose the realization of singular Jones metasurfaces through the zero of the Jones-matrix determinant (Fig. 1(a)). The scattering subspace is described by two orthogonal polarization states, such as left- and right-circular polarizations (LCP and RCP). Polarization tuning can address the singular Jones matrix response at the targeted eigen-polarization $\mathbf{E}_S = [-a\ c]^T$, with the outgoing field expressed as $\mathbf{E}_O = J\mathbf{E}_S$, where $J = \begin{bmatrix} a & b \\ c & a \end{bmatrix}$ is the reflective Jones matrix in the normal direction and the outgoing field $\mathbf{E}_O$ degenerates to a vectorial zero at the Jones singularity. This singular Jones response provides intrinsic polarization selectivity enabled by precise nanoscale engineering of plasmonic meta-structures (Fig. 1(b)).

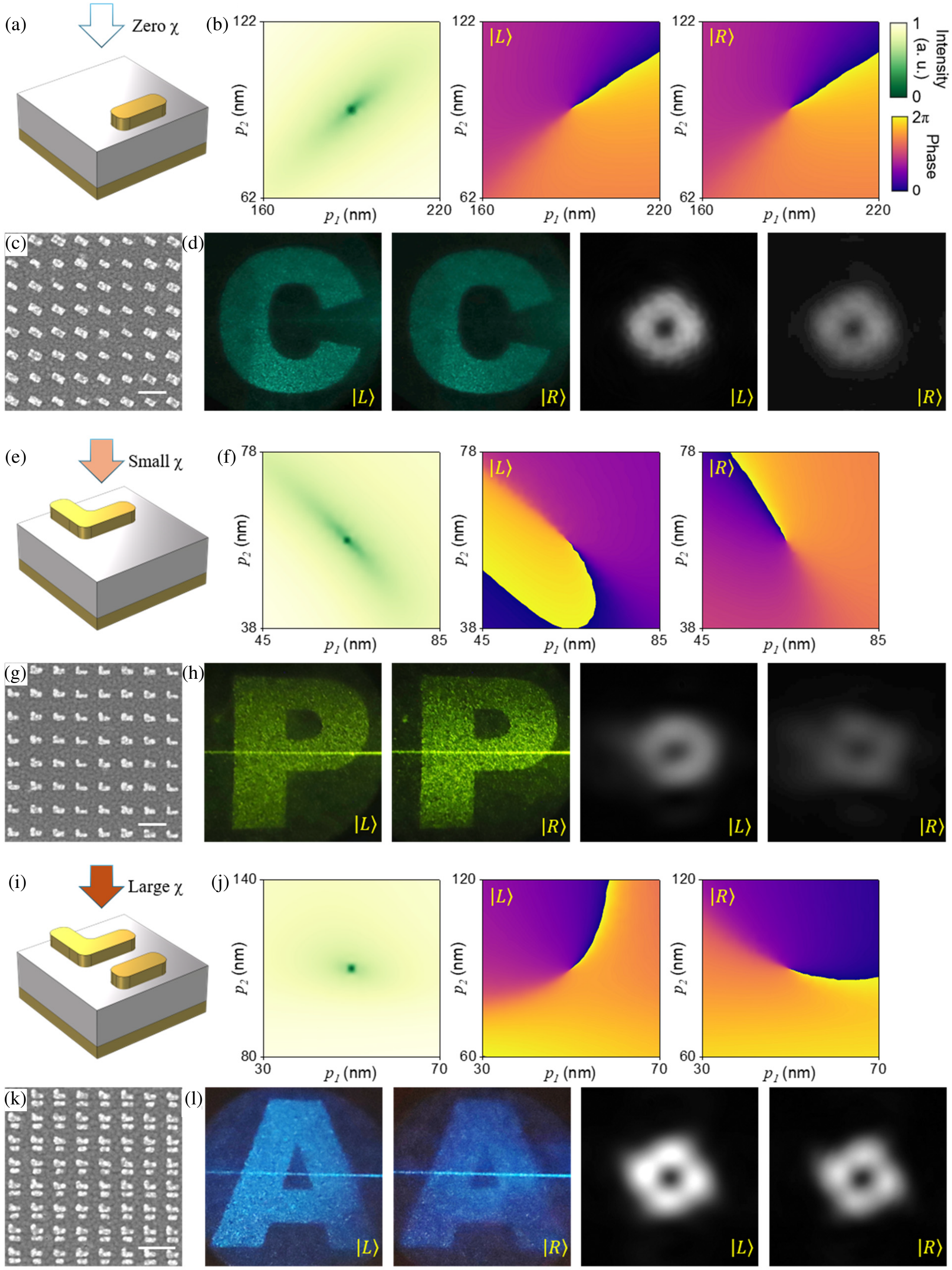

FIGURE 3. Simulated and experimental results of topological singular Jones metasurfaces. (a), (e), (i) Geometries for realizing singular Jones matrices with eigen-polarizations evolving from small to large ellipticity. (b), (f), (j) Simulated outgoing intensity under the incident eigen-polarization in 2D parameter space (p_1, p_2) and the outgoing topological phase under two orthogonal states. (c), (g), (k) Scanning electron microscope (SEM) images of the fabricated plasmonic metasurfaces. Scale, 500 nm. (d), (h), (l) Experiments on meta-holograms and vortex generation under two orthogonal states using the topological nature of the Jones-matrix singularity. The parameter space of (p_1, p_2) in (a) is the length and width of rod, (e) is the short length and width of L shape, and (i) is short length of L and length of rod.

By tailoring the anisotropy, inter-element coupling, and orientation of the plasmonic meta-atoms, the amplitude and phase of the reflection coefficients are adjusted to satisfy the singular condition of the Jones matrix of $\det(J) = 0$. At this point, a nonzero incident polarization eigenstate is mapped to a vectorial zero output, defining the singular Jones response. To

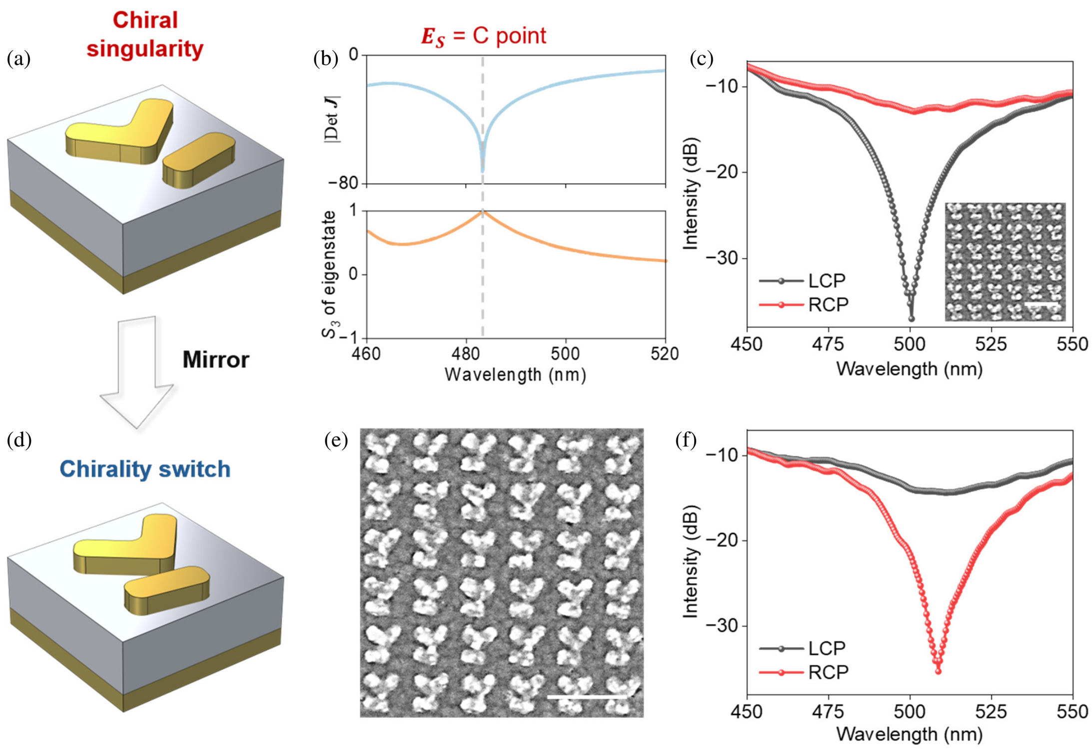

FIGURE 4. Chiral singular Jones metasurfaces. (a), (d) Structure layout and its mirror-symmetric counterpart of chiral singular Jones metasurfaces. (b) Simulated spectrum of Jones-matrix determinant showing a C-point eigen-polarization. (c) Measured spectrum of outgoing intensity for the chiral Jones singularity. Inset shows SEM image of the fabricated sample. Scale, 500 nm. (e) SEM image of the mirror-symmetry sample. Scale, 500 nm. (f) Measured spectrum of the switched chiral Jones singularity at the opposite handedness.

demonstrate polarization addressability of zero-output eigen-polarization states, we constructed various plasmonic geometries as shown in Fig. 2. With a single rod per unit cell and normal incidence as shown in Fig. 2(a), the singular matrix condition of $\det(J) = 0$ requires the two components to satisfy $|a| = |c|$ and therefore yields a linear eigen-polarization, which can be further tuned through the geometric phase. Ideally, changing the rotation introduces a relative phase shift between the cross-polarization components, so the eigen-polarization completes one azimuthal loop on the Poincaré sphere. In practice, deviations from this ideal trajectory may arise from more subtle interactions, such as orientation-dependent local responses and inter-cell coupling. In Fig. 2(b), an L shape slightly disrupts the coupling of $|a| = |c|$, resulting in a small ellipticity in the zero-output eigen-polarization. The coupled rod-L shape geometry induces a larger coupling breaking bringing the eigen-polarization closer to circular polarization as shown in Fig. 2(c). To approach the circular polarization (C point), we rotate the rod and L shapes and observe an extreme coupling-breaking case where $a \to 0$, forming a chiral Jones singularity as shown in Fig. 2(d) (see Supplementary Materials). We thus engineer the eigen-polarization to address the top hemisphere of the Poincaré sphere, while the bottom hemisphere can be realized through structural mirror symmetry. In our simulation, a zero-valued Jones-matrix determinant is observed for each plasmonic geometry as shown in Figs. 2(e)–(h), respectively, confirming the singular response in the Jones system. The corresponding Jones-matrix components are shown in Supplementary Fig. S1, where the individual components generally remain nonzero, but their interaction leads to deep zero output. This is the key characteristic of a Jones singularity that distinguishes it from conventional scalar scattering zero. The slight- and strong-decoupling cases represent two representative latitudes along a geometry-mediated coupling-tuning path, where varying the coupling modifies the relative strength and phase delay, thereby moving the eigen-polarization through the intermediate region of the Poincaré sphere.

The singular Jones response originates from the singularity of the Jones matrix and exhibits a robust twofold topological nature. The zero-output response acts as a vectorial zero, meaning that both field components vanish simultaneously in two orthogonal bases. When projected onto the two bases, this vectorial zero appears as a phase singularity in each component, thereby producing a twofold topology. Using three different geometries with distinct eigen-polarizations (Figs. 3(a), (e), (i)), ranging from small to large ellipticity χ, we show the emergence of outgoing vectorial zeros in a 2D parameter space with $(p_1,\ p_2)$ representing two structural parameters of the meta-atoms. When projected onto right- and left-circular polarization states, as used in the experimental polarization-detection process, the reflection exhibits topological phases with 2π winding around the singularity in both orthogonal channels, as shown in Figs. 3(b), (f), (j). This enables the exploitation of meta-hologram and vortex generation using dual nontrivial phases from the singularity [4, 5, 39], with robust functionality even when evaluated at two orthogonal states. Holographic images of letters "C", "P", and "A" are encoded into three samples using the Gerchberg-Saxton algorithm with the corresponding scanning electron microscope images shown in Figs. 3(c), (g), (k), respectively. In experiments, by shining the targeted zero-output eigen-polarizations (see Supplementary Fig. S2), meta-holograms of "C", "P", and "A" are retrieved at two circular states of $\{R, L\}$ in Figs. 3(d), (h), (l). Phase vortices of charge 2 are also demonstrated through three phase-winding samples. This verifies the topological singular Jones response and its distinctive twofold topology under two orthogonal states induced by the vectorial zero.

By breaking the Jones-matrix coupling to the maximum condition, a chiral singular Jones metasurface can be realized as shown in Fig. 4(a) (see Supplementary Fig. S3). We simulated the matrix determinant spectrum and the corresponding evolution of the Stokes parameter S_3 of the eigen-polarization as a function of wavelength (Fig. 4(b)). At the chiral singularity near 483 nm, the S_3 value approaches 1, indicating near-complete absorption of the LCP incidence. We also note that this corresponds to an exceptional point in the Jones matrix, where both eigenvalues coalesce to zero (see Supplementary Materials and Supplementary Figs. S4–S5). Experimentally measured reflected outgoing power confirms the chiral Jones singularity under normal incidence, with a dip observed in LCP intensity (Fig. 4(c)). Chirality switching is achieved through structural mirror symmetry (Fig. 4(d)), with the fabricated sample shown in Fig. 4(e). The switched chiral Jones singularity is experimentally confirmed through the measured spectrum, which shows a dip in RCP in Fig. 4(f). Ideally, mirror symmetry reverses the handedness of the chiral Jones singularity without shifting its resonance wavelength. The observed shift is mainly attributed to fabrication differences between the two samples, such as linewidth variations, edge roughness, corner rounding, and lift-off morphology, which slightly modify the plasmonic resonance and the amplitude–phase balance.

3. CONCLUSION

In conclusion, we propose and experimentally demonstrate polarization-addressable singular Jones metasurfaces with tailorable eigen-polarizations by engineering plasmonic structures. Matrix-level singular responses offer a distinct platform for harnessing topology and chirality. By incorporating both polarization and spatial degrees of freedom, polarization-selective vectorial extinction provides a versatile platform for controlling light beyond scalar singularities. Our work may advance topological wavefront shaping, polarization-addressed singular optics, and chiral absorbing platforms, while bridging metasurface engineering and non-Hermitian photonics. Future efforts may extend this framework to low-loss dielectric or hybrid platforms, active and reconfigurable metasurfaces [40], full Jones-matrix reconstruction, and applications in polarization-multiplexed wavefront shaping [41], chiral sensing, and compact singular photonic devices.

EXPERIMENTAL SECTION

Numerical simulations. The complex-valued Jones matrix of nanostructures is simulated with finite-element method. Periodic boundary conditions are applied, and perfectly matched layers are employed to absorb the outgoing waves. The refractive index of aluminum is taken from experimentally measured results. The reflected co-polarization and cross-polarization components are calculated by injecting circularly polarized light and measuring the reflected S parameters versus wavelength. To evaluate the existence of a singular matrix, Jones-matrix determinant is calculated and its zero indicates a singular condition. The corresponding eigenstate with zero eigenvalue is called the zero-output eigen-polarization of the singular Jones matrix.

Sample fabrication. The plasmonic metasurfaces for singular Jones responses are fabricated through standard clean-room procedures. First, a cleaned silicon wafer is precisely cut into square substrates with dimensions of 1×1 cm^2. Subsequently, a 150 nm thick layer of aluminum (Al) is deposited onto the substrate by means of thermal evaporation, which functions as the ground layer. After this, a 40 nm SiO_2 spacer layer is deposited onto the Al layer using magnetron sputtering. Next, a layer of CSAR 62 resist, approximately 120 nm thick, is spin-coated onto the spacer layer, and then baked at 180°C for 90 seconds to ensure proper adhesion and curing. The pattern exposure is carried out using electron-beam lithography (Elionix ELS-7500) at 50 kV, with the design being generated by the BEAMER-GenISys software. Once the pattern exposure is complete, the CSAR 62 resist is developed in ZED-N50 for 4.5 minutes, and then a 30-second IPA fixing process is applied to stabilize the pattern. Following this, a 30 nm Al layer is deposited through thermal evaporation. Finally, the fabrication process is completed with a lift-off step using Remover PG, and the fabricated metasurface is rinsed in IPA and deionized water to remove any residual chemicals, thus obtaining the desired metasurface.

Optical setup. During the measurement of holographic images and optical vortices, a laser beam with a specific wavelength passes through a linear polarizer and a quarter-wave plate. By adjusting the rotation angles of these two components, a customized incident polarization can be generated, which can be measured using a polarimeter (Thorlabs, PAX1000VIS). The beam is then weakly focused onto the metasurface using a lens with a focal length of 150 mm. Since the system operates in reflection mode, both the projection screen and the incident beam are positioned on the same side of the metasurface. The projection screen has a central hole that allows the incident light to pass through. To capture information from a specific polarization channel, a quarter-wave plate and a linear polarizer are placed in front of the holographic image. By altering their rotation angles, holographic images can be obtained under the desired polarization filtering condition. As for the chiral Jones singularity, the spectrum can be measured by replacing the single-wavelength laser beam with a supercontinuum light source (Anyang, SC-PRO-7) and directing the reflected light into a fiber-coupled spectrometer (Ocean Optics, Maya2000Pro).

ACKNOWLEDGEMENT

C.-W.Q. acknowledged the financial support by the Ministry of Education, Republic of Singapore (Grant No.: A-8002152-00-00 & A-8002458-00-00), and the Competitive Research Program Award (NRF-CRP26-2021-0004 & NRF-CRP30-2023-0003) from the National Research Foundation, Prime Minister's Office, Singapore. Q.S. acknowledged the funding support from the National Natural Science Foundation of China (12474388), Guangdong Basic and Applied Basic Research Foundation (2025A1515011483), Guangdong Provincial Department of Science and Technology (2023ZT10C040), Shenzhen Science and Technology Program (JCYJ20230807111706014). This work was also funded by the Basic Research Program of Jiangsu (BK20243029) and National Key Research and Development Program of China (2023YFF0613600).

REFERENCES

[1] Gbur, G. J., *Singular Optics*, CRC Press, 2016.

[2] Shen, Y., H. Wang, and S. Fan, "Free-space topological optical textures: Tutorial," *Advances in Optics and Photonics*, Vol. 17, No. 2, 295–374, 2025.

[3] He, C., Y. Shen, and A. Forbes, "Towards higher-dimensional structured light," *Light: Science & Applications*, Vol. 11, No. 1, 205, 2022.

[4] Song, Q., X. Liu, C.-W. Qiu, and P. Genevet, "Vectorial metasurface holography," *Applied Physics Reviews*, Vol. 9, No. 1, 011311, 2022.

[5] Song, Q., M. Odeh, J. Zúñiga-Pérez, B. Kanté, and P. Genevet, "Plasmonic topological metasurface by encircling an exceptional point," *Science*, Vol. 373, No. 6559, 1133–1137, 2021.

[6] Milione, G., H. I. Sztul, D. A. Nolan, and R. R. Alfano, "Higher-order Poincaré sphere, Stokes parameters, and the angular momentum of light," *Physical Review Letters*, Vol. 107, No. 5, 053601, 2011.

[7] Naidoo, D., F. S. Roux, A. Dudley, I. Litvin, B. Piccirillo, L. Marrucci, and A. Forbes, "Controlled generation of higher-order Poincaré sphere beams from a laser," *Nature Photonics*, Vol. 10, No. 5, 327–332, 2016.

[8] Ni, J., C. Huang, L.-M. Zhou, M. Gu, Q. Song, Y. Kivshar, and C.-W. Qiu, "Multidimensional phase singularities in nanophotonics," *Science*, Vol. 374, No. 6566, eabj0039, 2021.

[9] Liu, M., C. Zhao, Y. Zeng, Y. Chen, C. Zhao, and C.-W. Qiu, "Evolution and nonreciprocity of loss-induced topological phase singularity pairs," *Physical Review Letters*, Vol. 127, No. 26, 266101, 2021.

[10] Qin, H., Z. Yang, P.-S. Huang, X. Mu, S.-H. Huang, Y. Shi, W. Zhao, B. Li, J. Zhou, J. Zúñiga-Pérez, P. Genevet, P. C. Wu, and Q. Song, "Sphere of arbitrarily polarized exceptional points with a single planar metasurface," *Nature Communications*, Vol. 16, No. 1, 2656, 2025.

[11] Qin, H., Z. Su, Z. Zhang, W. Lv, Z. Yang, W. Chen, X. Gao, H. Wei, Y. Shi, B. Li, J. Zhou, R. Fleury, C.-W. Qiu, and Q. Song, "Disorder-assisted real-momentum topological photonic crystal," *Nature*, Vol. 639, No. 8055, 602–608, 2025.

[12] Li, T., M. Liu, J. Hou, X. Yang, S. Wang, S. Wang, S. Zhu, D. P. Tsai, and Z. Wang, "Chip-scale metaphotonic singularities: Topological, dynamical, and practical aspects," *Chip*, Vol. 3, No. 4, 100109, 2024.

[13] Yang, Z., P.-S. Huang, Y.-T. Lin, H. Qin, J. Zúñiga-Pérez, Y. Shi, Z. Wang, X. Cheng, M.-C. Tang, S. Han, B. Kanté, B. Li, P. C. Wu, P. Genevet, and Q. Song, "Creating pairs of exceptional points for arbitrary polarization control: Asymmetric vectorial wavefront modulation," *Nature Communications*, Vol. 15, No. 1, 232, 2024.

[14] Kim, D., A. Baucour, Y.-S. Choi, J. Shin, and M.-K. Seo, "Spontaneous generation and active manipulation of real-space optical vortices," *Nature*, Vol. 611, No. 7934, 48–54, 2022.

[15] Qin, H., Z. Zhang, J. Wang, and R. Fleury, "Topological hysteretic winding for temporal anti-lasing," *Nature Communications*, Vol. 16, No. 1, 6189, 2025.

[16] Lv, W., H. Qin, X. Shi, F. Shi, X. Mu, Z. Zhou, J. Qin, B. Li, C.-W. Qiu, and Q. Song, "Local-nonlocal assisted multifunctional photonic crystals," *Light: Science & Applications*, Vol. 15, No. 1, 243, 2026.

[17] Bliokh, K. Y., E. Karimi, M. J. Padgett, M. A. Alonso, M. R. Dennis, A. Dudley, A. Forbes, S. Zahedpour, S. W. Hancock, and H. M. Milchberg, "Roadmap on structured waves," *Journal of Optics*, Vol. 25, No. 10, 103001, 2023.

[18] Dorrah, A. H. and F. Capasso, "Tunable structured light with flat optics," *Science*, Vol. 376, No. 6591, eabi6860, 2022.

[19] Gao, X., Z. Yu, J. Yao, X. Mu, Y. Shi, P. Lai, B. Li, and Q. Song, "Discontinuous orbital angular momentum metasurface holography," *Nature Communications*, Vol. 16, No. 1, 10688, 2025.

[20] Yang, Z., P.-S. Huang, Y.-T. Lin, H. Qin, J. Chen, S. Han, W. Huang, Z.-L. Deng, B. Li, J. Zúñiga-Pérez, P. Genevet, P. C. Wu, and Q. Song, "Asymmetric full-color vectorial metaholograms empowered by pairs of exceptional points," *Nano Letters*, Vol. 24, No. 3, 844–851, 2024.

[21] Choi, E., G. Kim, J. Yun, Y. Jeon, J. Rho, and S.-H. Baek, "360° structured light with learned metasurfaces," *Nature Photonics*, Vol. 18, No. 8, 848–855, 2024.

[22] Zhang, X., Y. Liu, J. Han, Y. Kivshar, and Q. Song, "Chiral emission from resonant metasurfaces," *Science*, Vol. 377, No. 6611, 1215–1218, 2022.

[23] Chen, Y., H. Deng, X. Sha, W. Chen, R. Wang, Y.-H. Chen, D. Wu, J. Chu, Y. S. Kivshar, S. Xiao, and C.-W. Qiu, "Observation of intrinsic chiral bound states in the continuum," *Nature*, Vol. 613, No. 7944, 474–478, 2023.

[24] Duan, X., B. Wang, K. Rong, C.-l. Liu, V. Gorovoy, S. Mukherjee, V. Kleiner, E. Koren, and E. Hasman, "Valley-addressable monolayer lasing through spin-controlled Berry phase photonic cavities," *Science*, Vol. 381, No. 6665, 1429–1432, 2023.

[25] Guo, C., J. Li, M. Xiao, and S. Fan, "Singular topology of scattering matrices," *Physical Review B*, Vol. 108, No. 15, 155418, 2023.

[26] Baranov, D. G., A. Krasnok, T. Shegai, A. Alù, and Y. Chong, "Coherent perfect absorbers: Linear control of light with light," *Nature Reviews Materials*, Vol. 2, No. 12, 1–14, 2017.

[27] Pichler, K., M. Kühmayer, J. Böhm, A. Brandstötter, P. Ambichl, U. Kuhl, and S. Rotter, "Random anti-lasing through coherent perfect absorption in a disordered medium," *Nature*, Vol. 567, No. 7748, 351–355, 2019.

[28] Hu, H., C. Zhou, Y. Zhang, M.-X. Hu, J. Peng, H. Tang, L. Huang, J. Liu, C. Guan, Z. Zhu, *et al.*, "Robust chirality via merging accidental BICs with net zero topological charge," *eLight*, Vol. 6, No. 1, 12, 2026.

[29] Chong, Y. D., L. Ge, H. Cao, and A. D. Stone, "Coherent perfect absorbers: Time-reversed lasers," *Physical Review Letters*, Vol. 105, No. 5, 053901, 2010.

[30] Wan, W., Y. Chong, L. Ge, H. Noh, A. D. Stone, and H. Cao, "Time-reversed lasing and interferometric control of absorp-

tion," *Science*, Vol. 331, No. 6019, 889–892, 2011.

[31] Hörner, H., L. Wild, Y. Slobodkin, G. Weinberg, O. Katz, and S. Rotter, "Coherent perfect absorption of arbitrary wavefronts at an exceptional point," *Physical Review Letters*, Vol. 133, No. 17, 173801, 2024.

[32] Slobodkin, Y., G. Weinberg, H. Hörner, K. Pichler, S. Rotter, and O. Katz, "Massively degenerate coherent perfect absorber for arbitrary wavefronts," *Science*, Vol. 377, No. 6609, 995–998, 2022.

[33] Galiffi, E., A. C. Harwood, S. Vezzoli, R. Tirole, A. Alù, and R. Sapienza, "Optical coherent perfect absorption and amplification in a time-varying medium," *Nature Photonics*, Vol. 20, 163–169, 2026.

[34] Wang, Z.-Q., Y.-M. Sun, Y.-D. Hu, Y.-P. Wang, R.-C. Shen, W.-J. Wu, and J. Q. You, "Enhancement of signal-to-noise ratio at a high-order exceptional point of coherent perfect absorption," *Nature Communications*, Vol. 17, No. 1, 3343, 2026.

[35] Li, J., A. Jana, Y. Yuan, K. Zhang, S. N. Burokur, and P. Genevet, "Exploiting hidden singularity on the surface of the Poincaré sphere," *Nature Communications*, Vol. 16, No. 1, 5953, 2025.

[36] Oh, D., S. Baek, S. Lee, K. Lee, J. Park, Z. Liu, T.-T. Kim, and B. Min, "Complete asymmetric polarization conversion at zero-eigenvalue exceptional points of non-Hermitian metasurfaces," *Nanophotonics*, Vol. 13, No. 24, 4409–4416, 2024.

[37] Kang, M., Z. Zhang, T. Wu, X. Zhang, Q. Xu, A. Krasnok, J. Han, and A. Alù, "Coherent full polarization control based on bound states in the continuum," *Nature Communications*, Vol. 13, No. 1, 4536, 2022.

[38] Wang, C., W. R. Sweeney, A. D. Stone, and L. Yang, "Coherent perfect absorption at an exceptional point," *Science*, Vol. 373, No. 6560, 1261–1265, 2021.

[39] Yu, N., P. Genevet, M. A. Kats, F. Aieta, J.-P. Tetienne, F. Capasso, and Z. Gaburro, "Light propagation with phase discontinuities: Generalized laws of reflection and refraction," *Science*, Vol. 334, No. 6054, 333–337, 2011.

[40] Gu, T., H. J. Kim, C. Rivero-Baleine, and J. Hu, "Reconfigurable metasurfaces towards commercial success," *Nature Photonics*, Vol. 17, No. 1, 48–58, 2023.

[41] Zhang, Z., L. Kong, L. Zhang, X. Pan, T. Das, B. Wang, B. Liu, F. Wang, I. Nape, Y. Shen, and A. Forbes, "Structured light meets machine intelligence," *eLight*, Vol. 5, No. 1, 26, 2025.